SAND99-0281 J

The influence of crystal structure on the lattice sites and formation energies of hydrogen in wurtzite and zinc-blende GaN

A. F. Wright

Sandia National Laboratories, Albuquerque, New Mexico 87185-1415

Charge-state calculations based on density-functional theory are used to study the formation energy of hydrogen in wurtzite and zinc-blende GaN as a function of Fermi level. Comparison of these results reveals notable differences including a 0.56 eV lower formation energy for H_2 in wurtzite, and different configurations for H_2 and H^- in the two crystal structures. Furthermore, H^+ is found to be equally stable at bond-centered and anti-bonding sites in wurtzite, whereas it is unstable at a bond-centered site in zinc blende. These differences are due to distinct features of the two crystal structures including: i) the lower symmetry of wurtzite which provides a wider selection of bonding sites for H^+, and ii) the existence of extended three-fold symmetric channels oriented along the *c*-axis in wurtzite which provide more favorable bonding configurations for H_2 and H^-. N-H^+ stretch-mode vibration frequencies, clustering of H^+ in *p*-type material, and diffusion barriers for H^- are also investigated in wurtzite GaN. A diffusion barrier of 1.6 eV is found for H^- in wurtzite GaN, significantly lower than a previous estimate, and a tendency for H^+ clustering in *p*-type material is found.

DISCLAIMER

This report was prepared as an account of work sponsored by an agency of the United States Government. Neither the United States Government nor any agency thereof, nor any of their employees, make any warranty, express or implied, or assumes any legal liability or responsibility for the accuracy, completeness, or usefulness of any information, apparatus, product, or process disclosed, or represents that its use would not infringe privately owned rights. Reference herein to any specific commercial product, process, or service by trade name, trademark, manufacturer, or otherwise does not necessarily constitute or imply its endorsement, recommendation, or favoring by the United States Government or any agency thereof. The views and opinions of authors expressed herein do not necessarily state or reflect those of the United States Government or any agency thereof.

DISCLAIMER

Portions of this document may be illegible in electronic image products. Images are produced from the best available original document.

Hydrogen is a common impurity in GaN films grown via metalorganic vapor-phase deposition (MOCVD) where it is introduced either from the source compounds or from H_2 when used as a carrier gas.[1] Hydrogen may also be introduced after growth for purposes of device isolation,[2] as a byproduct of various processing steps,[1] or simply to study its annealing behavior.[2-4] Understanding the annealing behavior of hydrogen in GaN is particularly important because either low-energy electron-beam irradiation[5] or a post-growth anneal step[6] is needed to dissociate Mg-H complexes, and activate *p*-type doping in MOCVD-grown material. Moreover, hydrogen is retained in GaN up to a temperature of approximately 900°C, and is therefore expected to play a significant role in nearly all processing stages of GaN-based devices.[7]

Because of its importance to emerging nitride-based technologies, hydrogen in GaN has been the focus of a number of recent experimental and theoretical studies. (See chapters 6 and 11 in Ref. 1 for reviews of theoretical and experimental work in this area.) Many questions remain unanswered, however, regarding topics such as the annealling behavior of hydrogen and its interaction with point and extended defects. A starting point for answering these questions can be provided by theoretical studies of hydrogen in defect-free GaN. Neugebauer and Van de Walle (NVdW) performed such a study for zinc-blende GaN.[8, 9] They found several interesting features including a large negative-U effect and a preference for the nitrogen anti-bonding site by H^+ instead of the bond-centered site favored in other semiconductors. Based on their previous studies of native point defects in GaN,[10] they also suggested that hydrogen should display similar behavior in the more technologically relevant wurtzite structure. However, there are notable differences in the two crystal structures that could affect interstitial hydrogen (see also Chap. 6 in Ref.1). The lower symmetry of wurtzite, for instance, results in there being two different Ga-N bond lengths and bond angles. This could affect the relative stabilities of anti-bonding and bond-centered sites. An even more noticeable difference is revealed by examining the two crystal

structures on a length scale larger than their bond lengths. As shown in Fig. 1, the wurtzite structure has three-fold symmetric (trigonal) channels oriented along the [0001] direction (*c*-axis) and extending through the length of the crystal. In zinc blende, the analogous trigonal channels are oriented along <111> directions, but are blocked at intervals of 7.8 Å by a pair of gallium and nitrogen atoms. This structural difference is a direct result of the different stacking sequences exhibited by wurtzite and zinc blende along the [0001] and [111] directions, respectively (see Fig. 2).

To provide a starting point for understanding the behavior of hydrogen in wurtzite GaN and to investigate the structural differences outlined above, we have performed charge-state calculations for hydrogen in wurtzite and zinc-blende GaN. These calculations employed the Vienna *ab initio* simulation package[11] (VASP) utilizing ultrasoft pseudopotentials[12] within the framework of the Kohn-Sham formulation of density-functional theory.[13] The gallium and nitrogen atoms were modeled using pseudopotentials developed by Grossner *et al.*,[14] treating the Ga 3*d* electrons as valence, and the hydrogen atoms were modeled using the 200 eV set of pseudopotentials from the VASP database. Test calculations using gallium and nitrogen pseudopotentials from the VASP database yielded identical results to those obtained with the Grossner *et al.* pseudopotentials. We also performed test calculations using the generalized-gradient approximation (GGA) for exchange and correlation.[15] The results were the same as those obtained using the local-density approximation (LDA),[16] except for a pressure effect to be discussed further below.

We modeled hydrogen in GaN using periodically repeated 72-atom wurtzite and 64-atom zinc-blende supercells. Test calculations using a 32-atom zinc-blende supercell were performed to check the convergence of the 64-atom-cell results. No differences were found. Brillouin-zone sampling was accomplished using Monkhorst-Pack[17] parameters {222} which tests indicated was adequate for our purposes. We note that calculations for

bulk zinc-blende GaN yielded lattice constant 4.463 Å, and calculations for wurtzite yielded lattice parameters a = 3.157 Å, c = 5.145 Å, and u = 0.3765. These values are about 1% below measurements, typical of well-converged DFT-LDA calculations.[18]

Structures containing hydrogen were relaxed using the medium setting in VASP until the forces on each atom were less than 50 meV/Å. (Test calculations using the high setting in VASP yielded identical results.) Formation energies were obtained using the expression[19]

$$E^f(q,E_F) = E_{tot}(q) - n_{GaN}\mu_{GaN} - n_H\mu_H + qE_V + qE_F. \quad (1)$$

Here, E^f is the formation energy, E_{tot} is the energy of the supercell containing hydrogen, $n_{GaN}\mu_{GaN}$ is the energy of the supercell without hydrogen, n_H is the number of hydrogen atoms and μ_H is the hydrogen chemical potential, q is the charge state of the supercell, and E_V is the energy of the valence-band maximum in bulk GaN including a supercell-dependent shift.[19] E_F is the Fermi level defined to be zero at the bulk valence-band maximum and have a maximum value equal to the measured energy gap (3.25 eV for zinc blende and 3.48 eV for wurtzite). For μ_H, we used -0.90 eV which is the calculated spin-polarized energy of a hydrogen atom. Formation energies are thus given with respect to hydrogen *atoms* in the gas phase. To reference instead to H_2 in the gas phase, add 2.31 eV to the formation energies corresponding to the calculated binding energy of H_2 including the zero-point vibrational contribution. Many possible sites for interstitial hydrogen were investigated and formation energies for the three species, H^+, H^0, and H^-, were calculated at each site. We also studied supercells containing two hydrogen atoms, in both associated (H_2) and unassociated ($2H^+$) configurations. In the latter case, goal was to examine the likelihood of H^+ clustering in *p*-type material. We first describe our results for cells

containing one hydrogen atom, and then discuss results for cells containing an additional hydrogen atom.

Due to the large difference in electronegativity between nitrogen and gallium, the bonding in GaN is partly ionic in nature. This ionicity is expected to have a significant effect on the formation energies and stable lattice sites of the charged species, H^+ and H^-. NVdW,[8, 9] for example, found that H^+ in zinc-blende GaN prefers to remain near the negatively charged nitrogen atoms and H^- prefers to sit as far as possible from nitrogen atoms. We find similar results for hydrogen in wurtzite GaN, but we also find noteworthy differences in the stable lattice sites between wurtzite and zinc blende.

The most significant difference is in the lattice site of H^+. In zinc blende, we find that the nitrogen anti-bonding (AB_N) site is more stable than the bond-centered (BC) site by 0.26 eV. Due to its lower symmetry, there are two types of nitrogen-anti-bonding and bond-centered sites in the wurtzite structure. We refer to these as $AB_{N,\parallel}$ and $BC_\parallel$ where the N-H^+ direction is parallel the *c*-axis, and $AB_{N,\perp}$ and $BC_\perp$ where the N-H^+ direction is roughly perpendicular to the *c*-axis. We find that the $AB_{N,\perp}$ and $BC_\parallel$ sites have the same formation energy, the $BC_\perp$ site is 0.16 eV higher, and the $AB_{N,\parallel}$ site is an additional 0.03 eV higher. Our results therefore indicate that the $BC_\parallel$ site is stable in wurtzite, whereas the BC site in zinc blende was unstable by 0.26 eV as compared to the AB site. We attribute the stability of the $BC_\parallel$ site in wurtzite to its increased flexibility in relaxing bond angles between the nearby gallium and nitrogen atoms. In particular, placing H^+ in a bond-centered site causes the nearby gallium atom to relax into a planar configuration with its remaining three nearest-neighbor nitrogen atoms radically changing the Ga-N bond angles. The wurtzite structure is more easily able to relax its bond angles as was shown in a previous study of zinc-blende and wurtzite GaN elastic properties.[20] (See also Ref. 21 and Chap. 6 in Ref.1.)

The most stable site for H^- is also different in wurtzite and zinc blende. In zinc blende, H^- is stable at the gallium anti-bonding (AB_{Ga}) site, although the tetrahedral gallium ($T_{d,Ga}$) site is only 0.08 eV higher in energy. In wurtzite, the stable site is at the center of the trigonal channel (see Fig. 1), 0.66 Å from a plane of gallium atoms and roughly halfway between two planes of nitrogen atoms (see Fig. 2). The wurtzite analog to the zinc-blende $T_{d,Ga}$ site has a formation energy 1.76 eV higher than the trigonal site due to the presence of a nearby nitrogen atom. In general, the extended trigonal channel is an important structural feature distinguishing wurtzite from zinc blende. As noted above, the trigonal channel in zinc blende are blocked at intervals of 7.8 Å by a pair of gallium and nitrogen atoms. This blockage might also be expected to affect the diffusion barrier of H^- in zinc-blende GaN. In wurtzite, a likely diffusion path for H^- is along the center of the trigonal channel. Based on calculations for this path, we estimate the diffusion barrier to be 1.6 eV. The analogous path in zinc blende is from a $T_{d,Ga}$ site to a tetrahedral nitrogen ($T_{d,N}$) site, and then to a different $T_{d,Ga}$ site. The energy barrier for this path is estimated to be 1.9 eV, about 20% higher than the wurtzite result. We note that both of these values are significantly lower than the 3.4 eV given by NVdW.[8, 9] In particular, we do not see the sharp rise in energy shown in Fig. 1b of Ref. 9 near the midpoint of the path described above. The much smaller diffusion barriers found in this study imply that H^- will have noticeable mobility in GaN at growth and processing temperatures. A barrier of 3.4 eV, on the other hand, implies that H^- is practically immobile at these temperatures. We note that diffusion barriers for H^+ in GaN are more difficult to calculate, but are expected to be much lower than the 1.6 and 1.9 eV found above for H^- diffusion. These calculations are underway and will be reported elsewhere.

The very different H^- diffusion barriers found for zinc blende in our study and that of NVdW could be due to differences in details of our calculations. In particular, NVdW

treated the Ga 3*d* electrons as core[8, 9] whereas we have treated them as valence. Treating the 3*d* electrons as core can affect calculations involving interstitial hydrogen because the H 1*s* level lies near the Ga 3*d* levels in DFT-LDA calculations. As such, hybridization can occur between the Ga 3*d* and H 1*s* states, a feature absent when the 3*d* electrons are treated as core. Another effect arises because of the different lattice constants obtained when treating the Ga 3*d* electrons as core and valence. Treating the 3*d* electrons as core typically yields lattice constants 3-4% below measured values, whereas lattice constants are about 1% below measured values when the 3*d* electrons are treated as valence. The smaller lattice constant has the effect of applying pressure to the interstitial hydrogen atom, raising its formation energy. Test calculations with the Ga 3*d* electrons treated as core indicate that the first effect increases the diffusion barrier by about 0.25 eV and the second effect increases it another 0.15 eV when the lattice is compressed by 3%. Thus, these effects do not completely account for our different diffusion barriers and the source of the difference remains an open question. Before continuing, we note that the effect of pressure was also observed in our test calculations using the GGA form of exchange and correlation. Bulk lattice constants in this case are about 0.8% larger than measured values and the hydrogen formation energies are slightly lower as a result.

Due to its neutrality, NVdW found that the formation energy of H^0 in zinc-blende GaN was rather insensitive to position.[8, 9] We find the same insensitivity for H^0 in zinc-blende and wurtzite GaN. However, we observe that the formation energy of neutral H_2 is very sensitive to position and the stable sites are also quite different in the two crystal structures. In wurtzite, the stable site is at the center of the trigonal channel with the H-H bond parallel to the *c*-axis. One of the hydrogen atoms sits 0.45 Å from a plane of gallium atoms, the other sits 0.77 Å from a plane of nitrogen atoms, and the H-H bond length is 0.76 Å. In zinc blende, H_2 sits near a $T_{d\text{-}Ga}$ site in the trigonal channel with the H-H bond parallel to a <111> direction. One hydrogen atom sits 0.12 Å from a plane of gallium

atoms, the other sits 1.09 Å from a plane of nitrogen atoms, and the H-H bond length is again 0.76 Å. In wurtzite, H_2 is located roughly equidistant between planes of gallium and nitrogen atoms. In zinc blende, H_2 cannot sit at this same position because a nearby gallium atom is blocking the trigonal channel. As a consequence of these different positions, the H_2 formation energy in wurtzite is 0.56 eV lower than in zinc blende. The increased stability in wurtzite is likely due to a polarization of the molecule, and the resulting attractive dipole interaction with the three three nearby Ga-N pairs lining the trigonal channel. Polarization is not effective in zinc blende because the gallium atom blocking the trigonal channel would have the same charge as the nearby hydrogen atom.

In Fig. 3, we plot formation energies for the most stable sites in zinc blende and wurtzite as a function of Fermi level. The two plots are similar to each other and to the plot shown earlier by NVdW.[9] Both plots in Fig 3, for example, display large negative-U values of -1.8 eV for wurtzite and -2.2 eV for zinc blende, similar to the -2.4 eV reported by NVdW. (The U value is given as difference in crossing points of the H^0/H^- and H^+/H^0 formation energies, i.e., the difference in thermal ionization energies.) Our H_2 formation energy is about 0.6 eV lower than the value found by NVdW, however it is difficult to trace the origin of this difference as they did not specify the stable H_2 site.

A feature worth noting in Fig. 3 is the relatively low formation energy of H_2. Its value, given per atom in the plot, is the lower than those of H^+ and H^- when the Fermi level lies near the middle of the gap. This will not be significant in material where the hydrogen concentration is small compared to those of other impurities, or native defects. However, in where the hydrogen concentration is large (hydrogen-implanted material, for example), the low formation energy of H_2 may lead to noticeable effects. In particular, if hydrogen is the dominant impurity, then the Fermi level will be pinned roughly near the middle of the gap[4] yielding a non-negligible concentration of H_2. Another situation where the low formation

energy may become significant is in the growth of magnesium doped *p*-type material. Hydrogen acts like a donor in *p*-type material and will therefore compensate magnesium, lowering its formation energy. This compensation, however, tends to shift the Fermi level toward the middle of the gap[22] where H_2 can begin to form, limiting the concentration of H^+. Detailed calculations to investigate the interplay of Mg, H^+, and H_2 concentrations as a function of temperature would be useful in elucidating the optimum hydrogen concentration and temperature needed to achieve high levels of *p*-type doping.

For wurtzite GaN, we also estimated the vibration frequencies for N-H^+ stretch modes. The values are 3240 cm^{-1} for the $AB_{N,\parallel}$ site, 3120 cm^{-1} for the $AB_{N,\perp}$ site, 3680 cm^{-1} for the $BC_\parallel$ site, and 3480 cm^{-1} for the $BC_\perp$ site. As expected, the frequencies are higher for the bond-centered sites due to the repulsive interaction between the hydrogen atom and the nearby gallium atom having a broken bond. In addition, we note that these values are similar to those observed in hydrogen implanted material by Weinstein *et al.*[23] In that case, it was suggested that the vibrations corresponded to hydrogen passivating gallium-vacancy sites. Finally, we point out that the zero-point vibrational energy corresponding to these modes is approximately 0.2 eV. This contribution was not included in the formation energies shown in Fig. 3.

In addition to the calculations for neutral H_2, we also considered two H^+ ions in wurtzite GaN to assess the possibility of hydrogen clustering in *p*-type material. When separated by more than about 5 Å, the formation energy for the pair is simply the sum of the formation energies for two isolated H^+ ions, indicating that screening is effective in this system. Surprisingly, we also found several configurations, having H^+ ions bonded to the same or nearby nitrogen atoms, with formation energies equal to or lower than the sum of the formation energies for isolated ions. In addition to highlighting the effectiveness of screening in this system, these results suggest that either the strain fields surrounding two

H^+ ions can complement each other, lowering the total formation energy for the complex, or new bonds are being formed in the complex.

Three structures were found having formation energies lower than for isolated H^+ ions. The first has H^+ ions at consecutive $BC_{\parallel}$ sites along the [0001] direction. In this case, a new bond is formed from gallium and nitrogen atoms relaxing in opposite directions due to the presence of the H^+ ions. The second structure consists of H^+ ions at $BC_{\parallel}$ and $BC_{\perp}$ sites related to the same nitrogen atom. That is, the H^+ ions were found to break two Ga-N bonds on the same nitrogen atom, a result that indicates a strong reactivity for H^+ in GaN. The formation energies for these two configurations are 0.15 eV lower than for isolated H^+ ions in wurtzite GaN with the first structure likely benefiting from the formation of a new Ga-N bond and the second benefiting from complementary relaxations in the surrounding lattice. The third structure consists of H^+ ions in $BC_{\parallel}$ and $AB_{N,\parallel}$ sites in adjacent columns of atoms along the [0001] direction and lying roughly in the same plane perpendicular to the [0001] direction. The formation energy in this case is 0.31 eV below that for two isolated H^+ ions. The low formation energy is likely due to significant relaxation in the surrounding gallium and nitrogen positions. While we have not considered all possible configurations with two H^+ ions nor complexes containing more than two ions, these results suggest that hydrogen clustering may play a role in *p*-type material.

In summary, we find noteworthy differences in the formation energies and stable lattice sites of hydrogen in wurtzite and zinc-blende GaN. H^+ is equally stable at a bond-centered site and a nitrogen anti-bonding site in wurtzite GaN, but is unstable at a bond-centered site in zinc-blende GaN. This difference is attributed to the increased flexibility of wurtzite for relaxing Ga-N bond angles. Additional calculations for two H^+ ions in wurtzite GaN indicates that these ions can break two Ga-N bonds to the same nitrogen atom and, in general, can form clusters of several types. H_2 is found to have a lower formation energy in

wurtzite than in zinc blende, a result that could affect the growth of *p*-type wurtzite material. In *n*-type material, we find that H^- occupies different sites, and we estimate diffusion barriers of 1.6 eV in wurtzite and 1.9 eV in zinc-blende, significantly lower than the value given previously. In general, the different results for interstitial hydrogen zinc-blende and wurtzite GaN follow from differences in the two crystal structure related to the lower symmetry of wurtzite and the existence of trigonal channels in wurtzite extending through the length of the crystal. These structural differences are also likely to have an effect on the energetics of other types of interstitial atoms in zinc-blende and wurtzite GaN and on the energetics of other interstitial atoms interacting with hydrogen.[24]

I wish to thank Drs. S. M. Myers and J. S. Nelson at Sandia National Laboratories, Albuquerque for helpful discussions regarding this work. The *ab initio* total-energy and molecular-dynamics package, VASP, was developed at the Institute für Theoretische Physik of the Technische Universität Wien. This work was supported by the United States Department of Energy under Contract No. DE-AC04-94AL85000.

Sandia is a multiprogram laboratory operated by Sandia Corporation, a Lockheed Martin Company, for the United States Department of Energy under contract DE-AC04-94AL85000.

References

1 S. J. Pearton, in *Optoelectronic Properties of Semiconductors and Superlattices*, edited by M. O. Manasreh (Gordon and Breach Science, Amsterdam, 1997), Vol. 2.

2 S. C. Binari, H. B. Dietrich, G. Kelner, L. B. Rowland, K. Doverspike, and D. K. Wickenden, J. Appl. Phys. **78**, 3008 (1995).

3 S. J. Pearton, R. G. Wilson, J. M. Zavada, J. Han, and R. J. Shul, Appl. Phys. Lett. **73**, 1877 (1998).

4 S. M. Myers, J. Han, T. J. Headley, C. R. Hills, G. A. Petersen, C. H. Seager, W. R. Wampler, and A. F. Wright, submitted.

5 H. Amano, M. Kito, K. Hiramatsu, and I. Akasaki, Jpn. J. Appl. Phys. **28**, L2112 (1989).

6 S. Nakamura, T. Mukai, M. Senoh, and N. Iwasa, Jpn. J. Appl. Phys. **31**, L139 (1991).

7 S. J. Pearton, C. R. Abernathy, J. D. MacKenzie, U. Hömmerich, X. Wu, R. G. Wilson, R. N. Schwartz, J. M. Zavada, and F. Ren, Appl. Phys. Lett. **71**, 1807 (1997).

8 J. Neugebauer and C. G. Van de Walle, in *Materials Research Society Symposia Proceedings*, edited by S. Ashok, I. Akasaki, J. Chevallier and N. M. Johnson (Materials Research Society, Pittsburgh, Pennsylvania, 1995), Vol. 378.

9 J. Neugebauer and C. G. Van de Walle, Phys. Rev. Lett **75**, 4452 (1995).

10 J. Neugebauer and C. G. Van de Walle, in *Materials Research Society Symposium Proceedings*, edited by C. H. Carter Jr., G. Gildenblat, S. Nakamura and R. J. Nemanich (Materials Research Society, Pittsburgh, Pennsylvania, 1994), Vol. 339.

11 G. Kresse and J. Hafner, Phys. Rev. B **47**, 558 (1993); **49**, 14251 (1994); G. Kresse and J. Furthmüller, Comput. Mater. Sci. **6**, 15 (1996); Phys. Rev. B **54**, 11169 (1996).

12 D. Vanderbilt, Phys. Rev. B **41**, 7892 (1990).

13 W. Kohn and L. J. Sham, Phys. Rev. **140**, A1133 (1965).

14 U. Grossner, J. Furthmüller, and F. Bechstedt, Phys. Rev. B **58**, R1722 (1998).

15 J. P. Perdew, J. A. Chevary, S. H. Vosko, K. A. Jackson, M. R. Pederson, and D. J. Singh, Phys. Rev. B **46**, 6671 (1992).

16 D. M. Ceperley and B. J. Alder, Phys. Rev. Lett **45**, 566 (1980);); J. P. Perdew and A. Zunger, Phys. Rev. B **23**, 5048 (1981).

17 H. J. Monkhorst and J. D. Pack, Phys. Rev. B **13**, 5188 (1976).

18 A. F. Wright and J. S. Nelson, Phys. Rev. B **51**, 7866 (1995).

19 D. B. Laks, C. G. Van De Walle, G. F. Neumark, P. E. Blochl, and S. T. Pantelides, Phys. Rev. B **45**, 10965 (1992).

20 A. F. Wright, J. Appl. Phys. **82**, 2833 (1997).

21 M. A. Roberson and S. K. Estreicher, Phys. Rev. B **44**, 10578 (1991).

22 J. Neugebauer and C. G. Van de Walle, Appl. Phys. Lett. **68**, 1829 (1996).

23 M. G. Weinstein, C. Y. Song, M. Stavola, S. J. Pearton, R. G. Wilson, R. J. Shul, K. P. Killeen, and M. J. Ludowise, Appl. Phys. Lett. **72**, 1703 (1998).

24 F. A. Reboredo and S. T. Pantelides, submitted.

Figure captions

Figure 1. a) View of the zinc-blende structure along the [111] direction. b) View of the wurtzite structure along the [0001] direction (*c*-axis). Gallium atoms are shown as larger empty circles and nitrogen atoms as smaller filled circles.

Figure 2. a) View of the zinc-blende structure along the [110] direction. b) View of the wurtzite structure along the [11$\underline{2}$0] direction. Gallium atoms are shown as larger empty circles and nitrogen atoms as smaller filled circles.

Figure 3. Formation energies (per hydrogen atom) versus Fermi level in a) zinc-blende, and b) wurtzite GaN. *P*-type material corresponds to small values of the Fermi energy and *n*-type material to large values.

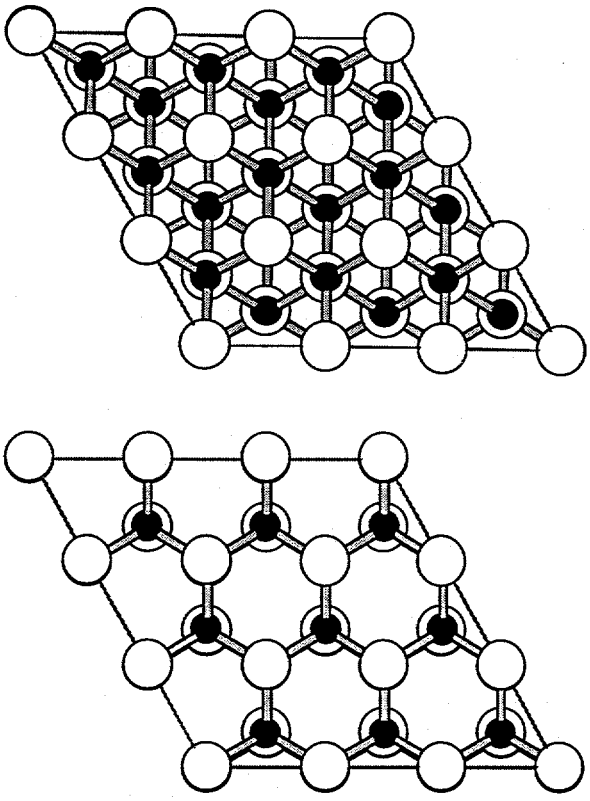

Fig. 1

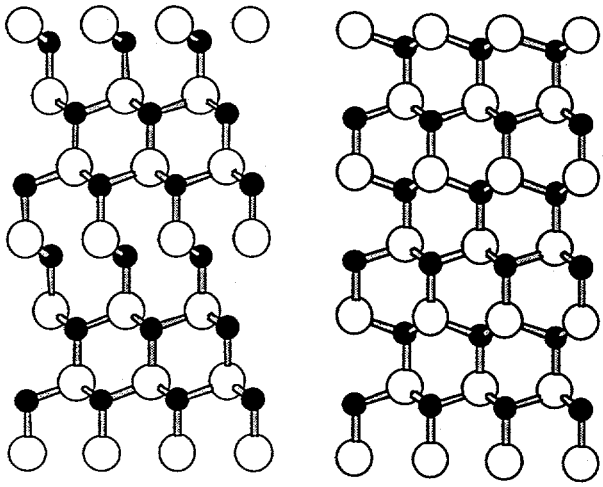

Fig. 2

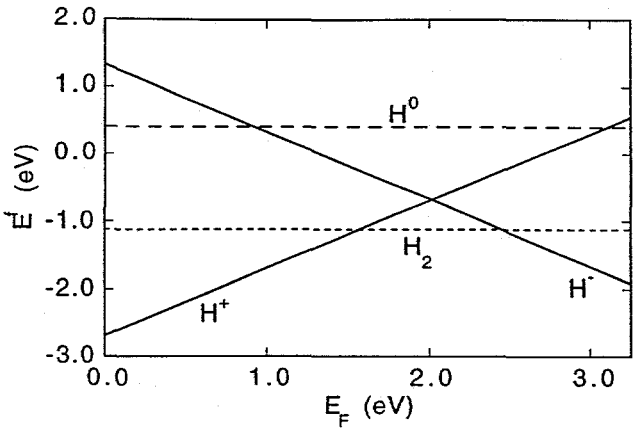
2.0
1.0
0.0
-1.0
-2.0
-3.0
E (eV)
H0
H2
H+
H-
0.0
1.0
2.0
3.0
EF (eV)

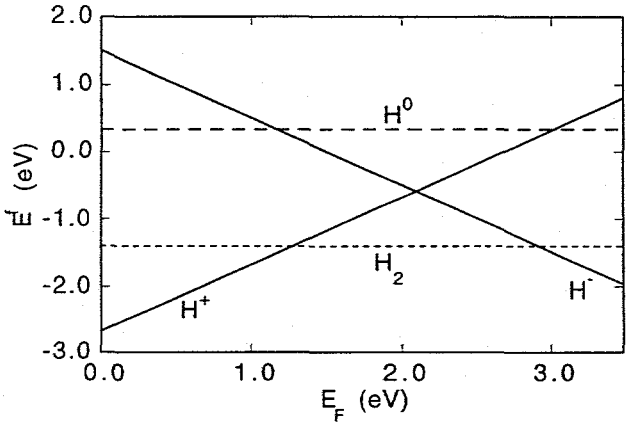
2.0
1.0
0.0
-1.0
-2.0
-3.0
E (eV)
H0
H2
H+
H-
0.0
1.0
2.0
3.0
EF (eV)

Fig. 3